J Mater Sci (2007) 42:4364–4371
DOI 10.1007/s10853-006-0631-5

The effect of microstructure and applied stress on magnetic Barkhausen emission in induction hardened steel

Mohamed Blaow · John Terence Evans · Brian A. Shaw

Received: 25 October 2005 / Accepted: 28 June 2006 / Published online: 28 February 2007

Abstract The influence of elastic deformation on the emission of magnetic Barkhausen noise (MBN) was investigated for induction-hardened low alloy steel with two different treatments: a standard temper (ST) and an over temper (OT) heat treatment. The rectified MBN profiles were found to be reversible with respect to loading and unloading, i.e., a profile that was changed by application of stress was recovered when the stress was removed. Characteristics of the profiles (peak height V_p, peak position I_p and half-width W_p) were recorded as a function of applied stressσ. Plots of V_p versus σ were S-shaped, with V_p reaching a maximum on the tensile side of the graph and a minimum on the compression side. In a more restricted stress range, between –500 and 1,000 MPa, V_p was an approximately a linear function of σ. The OT specimens showed greater sensitivity to stress than the ST specimens. Another difference was that the OT specimens produced an MBN profile with two overlapping peaks when under compression. The other profile characteristics showed a relationship with stress that ran counter to that of V_p, i.e., where V_p increased with increasing stress, I_p and W_p decreased. The observations are discussed in the light of established models of Barkhausen noise.

M. Blaow · J. T. Evans (✉) · B. A. Shaw
School of Mechanical and Systems Engineering, University of Newcastle upon Tyne, Newcastle upon Tyne NE1 7RU, UK
e-mail: j.t.evans@ncl.ac.uk

Introduction

Techniques based on the phenomenon of Barkhausen noise are potentially useful for non-destructive evaluation of ferromagnetic materials. For instance, residual tensile stress and over-tempering can be detected in ground-finished surfaces using measurements of magnetic Barkhausen noise (MBN) [1]. However, a large number of variables influence MBN emission and the technique produces only comparisons between different material states, e.g., for a given alloy, measurements have to be assessed against those for a specimen in a standard microstructural state for the alloy.

Barkhausen noise is produced by the irreversible movement of domain walls in a magnetisation cycle. Domain walls are pinned temporarily by microstructural barriers to their motion and then released abruptly in the changing magnetic field [2–4]. The resulting discrete changes in local magnetisation can be detected as voltage pulses in a search coil or magnetic read head. Precipitates, grain boundaries and dislocations act as effective barriers to domain wall motion so that MBN is sensitive to microstructure and plastic deformation. The influence of magnetostriction on magnetisation also makes emission sensitive to stress [3, 4].

The effect of applied and residual stresses on MBN emission has been presented in a number of studies (e.g., Refs. 3–22). However, stress, composition and microstructure interact to affect MBN [5–12]. Accordingly, it is useful to study the effect of applied stress on MBN in alloys with a range of compositions with different microstructures and with a range of mechanical strengths. The stress sensitivity of MBN in tension is found to be different to that in compression.

Sengupta and Theiner [8] found that the sensitivity to compression was higher than the sensitivity in tension. Lindgren and Lepisto [9] also found that the stress sensitivity to tension was lower than that in compression in non pre-strained mild steel but this was reversed with pre-strained material where the response to tension was found to be higher than the response to compression. MBN level versus stress in some cases showed linear relationship [11] where tension increased MBN level and compression decreased it. However, in many cases MBN versus stress shows a sigmoidal relationship where MBN level saturated at certain tensile and compression levels [10, 12]. It has also been reported that the MBN level increased with tensile stress, but reached a maximum at a particular stress value well below the yield point, after which it decreased with increasing stress [15–18]. With increasing compression, in most cases MBN level shows a decrease followed by saturation at higher compressive stresses. The many variations reported may be the result of differences in materials tested and the instrumentation used. Hyde et al. [12] produced calibration curves for a range of quenched and tempered steel, which showed increasing root mean square MBN output with increasing tensile stress. The stress sensitivity was found to be much higher in the over-tempered specimens than that in the standard tempered specimens.

Much of the work on the stress sensitivity of MBN emission has been done on mechanically soft steels. However, development of MBN as a non-destructive examination technique would be most usefully applied to case hardened steel components. Case hardening can be achieved by carburisation, requiring the diffusion of carbon into the surface layers to give a high carbon content, or by induction hardening, where no change in chemical composition is involved. The compositions of the steels used in these two processes are very different. In a previous paper [22], the present authors tested a fully hardenable steel, heat treated to give a very wide range of mechanical strength and hardness. That material was selected for testing because in the fully hardened state it corresponds closely in composition and properties to the surface layers in case-carburised steel components. Such material is used in many wear resistant engineering components such as small to medium size gears and bearings. Unfortunately, hardness, microstructure and stress state do not uniquely determine the MBN response of steel. MBN output is also sensitive to the particular composition of the steel [23]. For that reason there is also interest in results for steel of the induction hardening type. Induction hardening steels are used for larger engineering components and have a different composition to the case-carburising type of steels. They owe their high hardness and wear resistance to differential heating and quenching, rather than to a change in chemical composition in the surface layers. The authors previously presented results [24] for steel with the same composition as that used in the present work. However, at that time, for technical reasons we were not able to induction harden the test specimens and the results presented in Ref. [24] are for to softer material (300 kgf mm^{-2} VPN) more typical of the interior than the hardened surface layers found in real engineering components. The results in Ref. [24] also focussed on the effect of plastic deformation in bending and on the residual stresses induced by unloading from the elastic to plastic state. It is the object of the present paper to complete the picture for induction hardening steel by presenting results for specimens that were induction hardened to produce surface layers with high hardness (570–680 kgf mm^{-2} VPN). Because of the limited ductility of these specimens, the effect of elastic deformation only was examined.

Materials and method

Magnetic Barkhausen emission was recorded as a function of applied stress in bars loaded in cantilever bending. Test bars (100 mm × 10 mm × 10 mm) were machined from a plate of steel stock with the composition shown in Table 1. The material (commonly referred to as EN19 in the UK and equivalent to AISI/SAE 4140) is of commercial significance because it is widely used for the production of induction-hardened components, including large gears, where conventional heat treatment by quenching and ageing is impractical. Here, the surface layer is hardened by transient heating with induced high frequency currents followed by rapid cooling brought about by diffusion of heat from the surface layer into the bulk. The test bars used in the present experiments were induction hardened by a specialist company. The treatment produced material with a martensitic structure at the surface, whereas the bulk material, at depths of more than 1 mm below the surface, consisted of fine pearlite. One batch, identified by the label ST, was then tempered at 180 °C for 1 h (standard tempering for induction hardened gears).

Table 1 Composition of induction hardening steel

Element	C	Mn	Ni	Cr	Mo	Si	Cu	P	S
Wt. %	0.4	0.99	0.13	1.03	0.21	0.24	0.23	0.01	0.02

A second batch, identified by the label OT, was over-tempered at 300 °C for 2 h. Both treatments produced a tempered martensitic structure in the case region, examples of which are shown in Fig. 1. Microhardness profiles of ST and OT specimens are shown in Fig. 2. The treatments produce a hardness gradient below the surface but, as is typical with surface induction hardening, the material is reasonably homogeneous down to a depth of 1 mm below the surface. For the reasons discussed below, the MBN measurements reported below relate to the hardened material near the surface and the results are from an effectively homogeneous material. On the basis of previous measurements relating hardness and compression strength [22] the yield strength σ_0 of the ST and OT specimens is estimated to be 2,000 and 1,700 MPa, respectively. These values were used to ensure that the deformation, carried out by loading in bending, was limited to be within the elastic regime and to scale the applied stress in some of the graphs shown below.

Surface residual stresses were measured in the longitudinal direction after induction hardening and tempering using a Stresstech X3000 X-ray diffraction analyser. The values were –70 and –20 MPa for the ST and OT specimens, respectively. These values are low

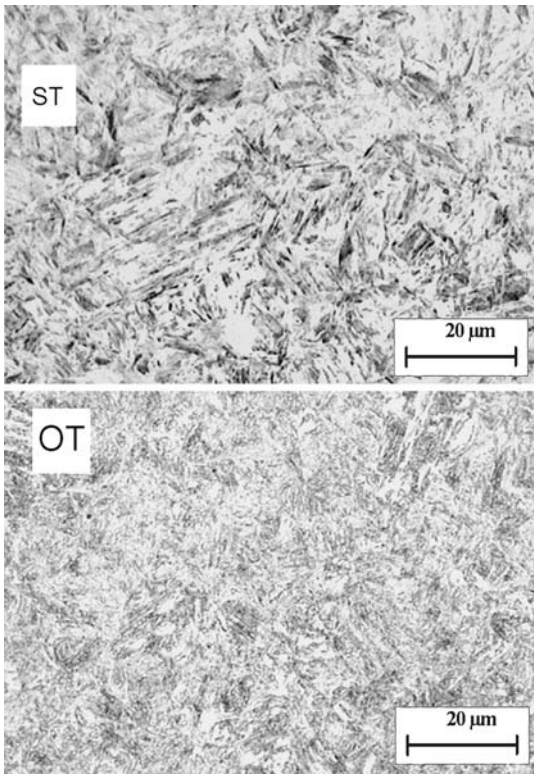

Fig. 1 Microstructures in specimens with two heat treatments: standard temper (ST) and over-tempered (OT)

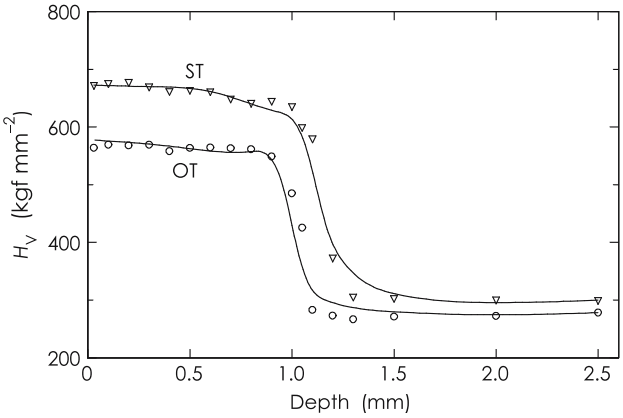

Fig. 2 Microhardness profiles for standard tempered (ST) and over-tempered (OT) specimens

compared with the range of applied stress used in the loading experiments. As a matter of interest, extensive testing for residual stress in induction hardened steel components shows that stresses in the case are usually modest and compressive. Larger (positive) stresses occur only at the case–core interface, which in the present instance would be more than 1 mm below the surface and would not perturb the measurements reported below.

To make MBN measurements as a function of applied stress, specimens were mounted in a rig with one end anchored en-castre in a rigid fixture and the other end attached to a long cantilever arm. This left 75 mm of the specimen exposed and accessible to the magnetising yoke that was orientated so that the magnetic field was parallel to the maximum principal stress direction. The applied moment was increased by applying masses to the free end of the cantilever. The effect of tensile stress on MBN was measured by attaching the magnetising yoke and search coil to the upper surface. The effect of tensile stress could then be compared with the effect of compressive stress of equal magnitude in each load step by relocating the MBN fixtures to the lower surface. As long as specimens remain elastic, the calculation of strain or stress in a beam is simple. The applied moment at which the outer fibres become plastic is given by the expression [25]

$$M_{\mathrm{Y}} = \frac{1}{6} b h^2 \sigma_0, \tag{1}$$

where σ_0 is the yield strength and h and b are the height and thickness of the beam, respectively. In the elastic regime, the ratio of surface applied stress to yield strength is given by

$$\sigma/\sigma_0 = M/M_Y\ , \quad (M < M_Y) \tag{2}$$

Cantilever bending was used to deform the test specimens because it is simple to apply and because it is appropriate for testing a wide range of materials at small strains. Unless elaborate precautions are taken, an un-quantified element of bending occurs in uniaxial loading owing to misalignment [26]. Thus, adopting bending as the main deformation mode avoids these errors and is a suitable method for stressing stiff materials with low ductility. It should also be noted that MBN emission samples a finite depth below the surface of the material [27], which, in bending, is subject to an inhomogeneous strain field. However, the relatively small sampling depth for MBN means that surface strain can be regarded as a characteristic of the deformation near that surface.

The MBN measurements were made using equipment developed in the authors' laboratory. The testing procedure was developed to give a high degree of reproducibility, i.e., to produce minimum variations in a run of tests on the same specimen. Since the MBN rig is relocated from the tension to the compression surface and back again in each load step, it is essential that the process of relocation did not itself produce significant variations in the recorded MBN profile. In developing the technique, a good deal of effort was expended in achieving this degree of reproducibility [23]. A schematic illustration of the equipment is shown in Fig 3. To produce a constant rate of magnetic induction in the specimen, the U-shape electromagnetic yoke is fed by a triangular waveform from a bipolar amplifier to take the specimen to near saturation at maximum current. A driving current, amplitude 1 A at a frequency of 0.2 Hz was used to produce a maximum magnetic field strength of 4.5 kA m^{-1}. A relatively low excitation frequency is used to minimise eddy current opposition to the applied magnetic field and to ensure a relatively slow magnetisation rate in the sample.

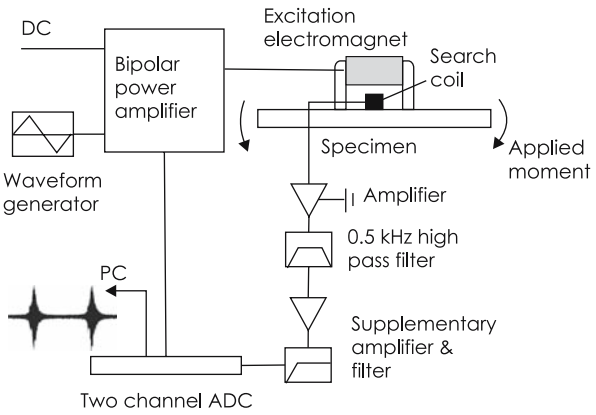

Fig. 3 Schematic layout of the MBN measurement apparatus

Barkhausen emission is detected by a search coil with 16×10^3 turns wound around a ferrite core. The signal is amplified in two stages. In the first stage, the gain is fixed at 40 dB. The amplified signal is filtered using a 3–100 kHz band pass filter. After filtering, the signal is passed through an additional amplifier with a variable gain of up to 60 dB. To minimise interference, the signal is finally passed to a 0.5 kHz high pass filter. The BN signal is then acquired using a 20 Ms/s Pico Tech 12-bit DAC oscilloscope and stored in a PC. It is convenient to smooth emissions to produce a measure of the amplitude of the envelope enclosing the signal. This is done numerically using a Matlab script. The signal is rectified by calculating the local root mean square for 100 successive points then smoothened using a digital filter for fifteen points.

As discussed below, to a first approximation, MBN emission is correlated with the differential permeability of the material, i.e., it is proportional to the instantaneous slope of the BH curve [3]. It follows that in a homogeneous material the emission is a maximum twice in each hysteresis loop. The intensity of the MBN emission is anticipated to peak at a positive field with increasing energising current and peak again at a negative field as the state of magnetisation of the sample moves around the BH loop. This was observed in our experiments, but only profiles obtained with a rising current are reported below.

Results

The effect of stress on the MBN profiles is relatively straightforward for the over tempered (OT) specimens stressed in tension and for the standard tempered (ST) specimens stressed in both tension and compression. In these cases, the application of stress simply changes the profile characteristics without changing the form of the profile. However, a more complicated effect appears in the OT material stressed in *compression*, where the presence of compressive stress induces two overlapping peaks in the MBN profile.

Examples of the effect of stress on MBN profiles are shown in Fig. 4a and b. The effect of increasing tension on the profiles obtained with the ST specimens is illustrated in Fig. 4a. Initially, the height of the peak increases with increasing stress, up to a value of σ equal to about $0.5\sigma_0$. The peak height then decreases with further increases inσ. The effect of compressive stress in producing a profile with two overlapping peaks in an

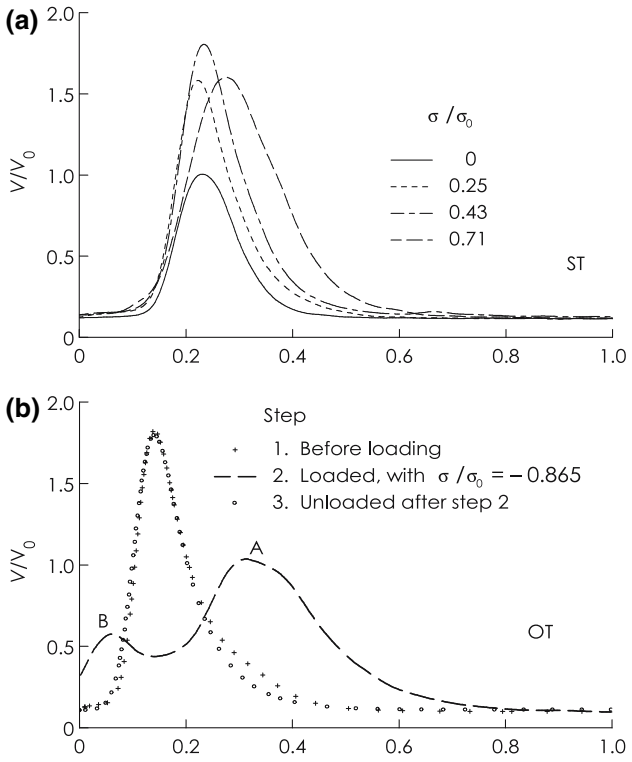

Fig. 4 Examples of MBN profiles. Effect of (**a**) tensile stress on a standard tempered (ST) specimen; (**b**) compressive stress on an over-tempered specimen. Reversibility with respect to loading and unloading is demonstrated in (**b**). The profile V is normalised with respect to the peak value V_0 of the ST specimen under zero stress

OT specimen is illustrated in Fig. 4b. The peaks at the higher and lower field values are labelled peak A and B, respectively.

It should be noted that the results reported here are sensibly reversible with respect to loading and unloading, i.e., a profile that is changed by application of stress is recovered when the stress is removed. This is particularly illustrated in Fig. 4b for a change involving the development of two overlapping peaks, although similar reversibility was found for all deformation in the elastic regime. In Fig. 4b, a broad MBN envelope with two peaks is strongly developed under a compressive stress $\sigma = -0.865\sigma_0$, but when the load is removed the initial single-peak profile is recovered.

In order to characterise the effect of applied stress on the MBN profiles, three parameters were measured as indicated in Fig. 5. V_p is the height of the peak and the peak position I_p is the value of the energising current at which the peak occurs. The peak half-width W_p is the width of the profile at half the peak height.

Peak height V_p was tabulated as a function of the applied stress σ. For convenience, V_p is normalised with respect the peak height V_0 of the ST specimen at zero stress and plotted against the dimensionless ratio σ/σ_0 in Fig. 6a. In the range $-0.2 < \sigma/\sigma_0 < 0.3$, the peak height is an approximately linear function of stress. At higher stresses, the peak height reaches a maximum and then falls slightly with further increases in stress. At lower stresses, the peak height reaches a minimum and then increases slightly with increasing compression. The peak height is larger for the OT than for the ST specimens and the output from the OT specimens shows the greatest sensitivity to stress in the linear region.

The changes in peak position I_p with stress are shown in Fig. 6b. The peaks of the OT specimens occur at lower current values than those of the ST specimens. In addition there is a clear tendency for all the peaks to occur at higher current values as the compression increases.

Figure 6c shows that the MBN profiles are narrower for the OT specimens than for the ST specimens under tensile stress. However, the position is reversed when the applied stress is compressive. Clearly, the broadening of the MBN profile for the OT specimens in compression is associated appearance of two overlapping peaks in the profile (Fig. 4b).

A pattern is evident in Fig. 6a–c. Larger MBN peaks (V_p) are correlated with lower peak positions (I_p) and a narrower profile width (W_p). A similar pattern has been seen in experiments on other materials [22]. Possible underlying factors responsible for these correlations are discussed below.

Discussion

Barkhausen noise is a microscopic phenomenon with a stochastic character [2, 28]. However, Barkhausen emission is modulated by the effect of dynamic magnetic permeability and the presence of stress, which are macroscopic-scale quantities [3, 4, 29]. For instance, when emission is produced by the irreversible movement of domain walls, a peak occurs in the MBN profile in the magnetic cycle because the dynamic permeability also peaks in this way in the course of half a magnetic cycle. In this sense, the potential usefulness of MBN in non-destructive evaluation arises mainly from the interactive effects of the macroscopic parameters. As with previously reported results [22], the authors believe that the pattern of behaviour shown Fig. 6 can to a large extent be rationalised by considering the likely effects of stress and microstructure on the associated BH curves for the material.

Jiles [3] has reviewed theoretical models highlighting the connection between MBN and the irreversible

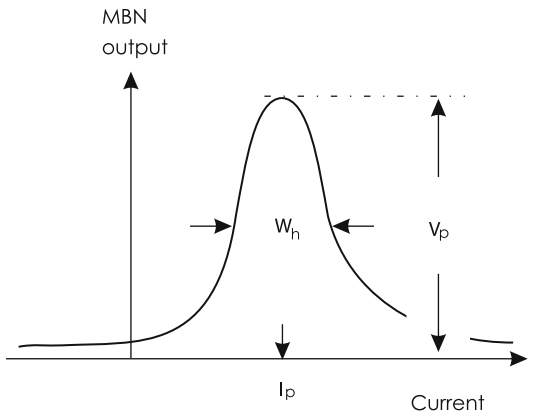

Fig. 5 Parameters used to characterise the profiles: peak height V_p, peak position I_p and half-width W_h

component of magnetisation M_{irr}. A basic assumption is that the intensity of emission is proportional to the differential susceptibility $\chi_{irr} = dM_{irr}/dH$, where H is the magnetic field. For the present discussion, it is convenient to recast this connection in terms of parameters obtained from the standard BH curve. This is not strictly accurate because the standard BH curve includes an element of reversible behaviour, but it is convenient to take this approach because the correlations between microstructure, stress and BH behaviour is generally known from the literature. Thus, in terms of the BH loop, we expect the intensity of emission to be (approximately) proportional to the differential permeability $\mu = dB/dH$. It follows that any changes in modulation of the MBN emission will reflect underlying changes in the BH loop. This can be understood with reference to the schematic diagram in Fig. 7. For instance, if the BH loop becomes narrower whilst retaining the same B value at saturation, one would expect the maximum value of μ to increase along with the peak emission. At the same time, one would expect the value of H at which the peak occurs to diminish along with the width of the MBN envelope. Conversely, if the BH loop becomes broader, the peak emission will diminish while the corresponding H value and profile width will increase.

In the experiments, the peak output V_p (Fig 6a) is larger for the OT than for the ST specimens, while the peak position I_p (Fig. 6b) is lower. On the above arguments, this is consistent with the idea that overtempering narrows the BH loop relative to that of the standard tempered material. Such a conclusion is consistent with what is known about the effect of microstructure on the BH loop [30], where the changes in microstructure that produce mechanical hardening (e.g., Fig. 2) also induce magnetic hardening. The

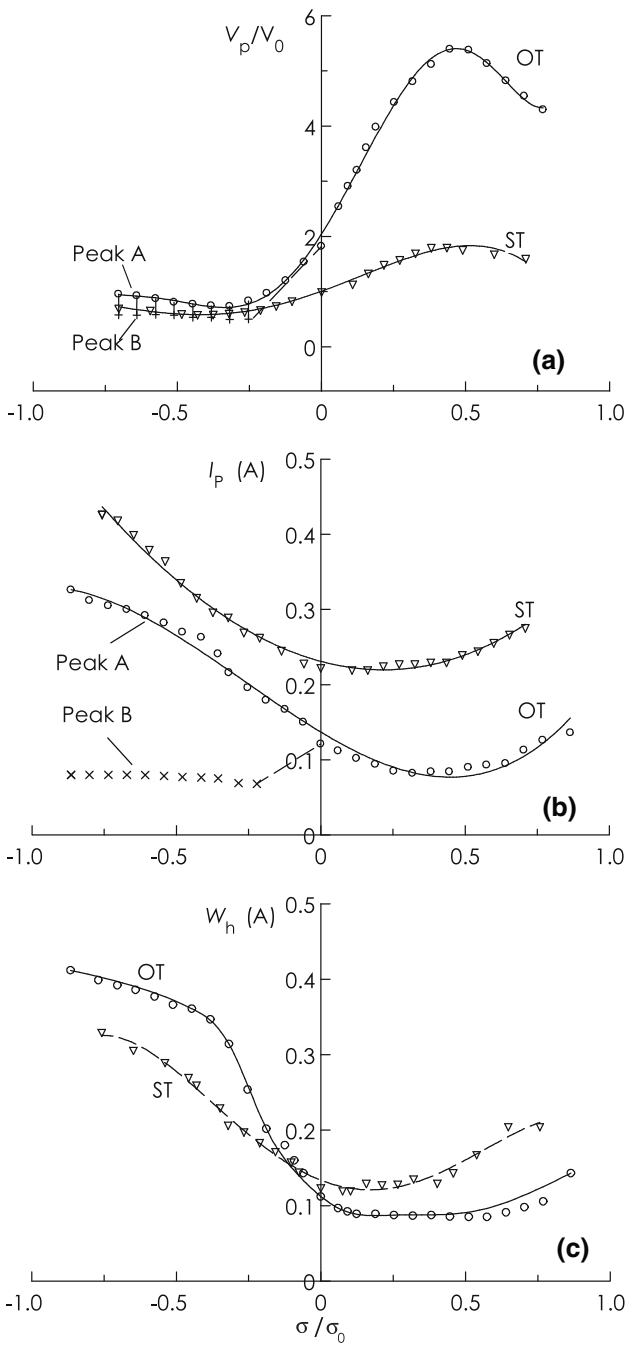

Fig. 6 The effect of applied stress on (**a**) peak height, (**b**) peak position and (**c**) half width. The circles show the results for peak A in the OT specimens. The results for peak B are indicated by crosses. Note that in (**a**) the points for peak B (OT specimen) are partly obscured by the points for the ST specimen. In the graphs, the applied stress σ is scaled with the yield strength σ_0 = 1,700 MPa for the OT specimens and 2,000 MPa for the ST specimens

behaviour of the half-width (Fig. 6c) is also consistent with this picture, but only at zero stress or in the tension region where single MBN peaks occur.

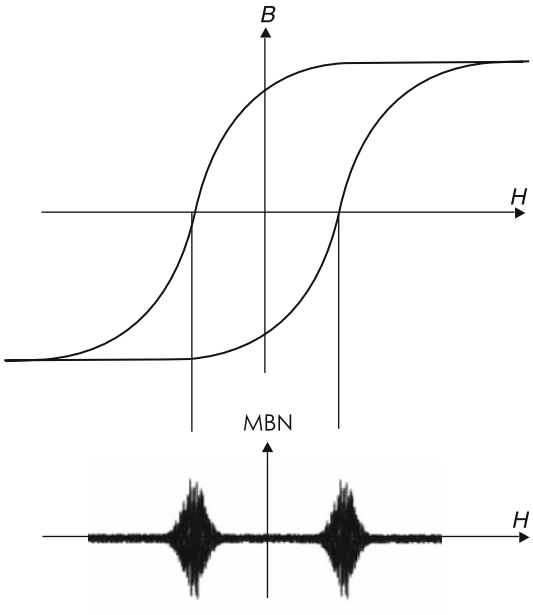

Fig. 7 Schematic illustration showing the connection between the BH loop and MBN emission

The effect of applied stress is somewhat complicated across the whole range. However, in the restricted range $-0.2\sigma_0 < \sigma < 0.4\sigma_0$, it can be seen that increasing σ increases V_p and reduces I_p and W_h. On the above arguments, this is consistent with the BH loop becoming narrower with increasing stress [31]. This behaviour is well known in materials with positive magnetostriction and Sablik and Jiles have given a quantitative account of the interacting factors in their magneto-elastic model [32].

At higher stresses ($\sigma > 0.5\sigma_0$), V_p reaches a maximum and then declines with further increases in stress (Fig. 6a). This downturn in V_p is accompanied by an upturn in peak position (Fig. 6b) and an increase in half width (Fig. 6c). Although this behaviour is not accounted for by the formal, quantitative theory, similar experimental observations have been reported for low carbon steels [15–18] and in medium carbon steel with spherodised carbides [22]. The connection here is that these materials are relatively soft (both mechanically and magnetically) and have a relatively high MBN output. In a previous paper [22] it was remarked that materials with a high MBN output at zero stress appear to have relatively little scope for further increase under tensile stress. In fact, this limited scope appears to be associated with a downturn in MBN output of the sort shown in Fig. 6a. The stress at which MBN shows a maximum has been designated by the label σ_{CB}. It has been proposed that because of stress induced anisotropy, the differential magnetostriction $d\lambda/dM$ becomes negative when $\sigma < \sigma_{CB}$ and that this is responsible for the fall in Vp at higher stress levels [15–18].

The peak position I_p increases with increasing compression (ST and OT Peak A), consistent with the idea that the BH loop becomes broader with increasing compressive stress. However, V_p reaches a minimum at about $\sigma = -0.25\sigma_0$, and remains virtually constant with further compression. The peak half-width behaviour breaks the suggested pattern in the compression regime because W_h is larger for the OT than for the ST specimens when $\sigma < -0.2\sigma_0$. However this reversal must be due to the appearance of the double peak profiles in the OT specimens under increasing compression. Possible mechanisms for the double-peak profiles are now discussed.

A notable feature of the results is the appearance of the double-peak profile in the OT specimens in compression. Overlapping peaks in MBN profiles have been reported by a number of workers [13, 17, 22, 32, 34]. One possible cause of overlapping peaks is inhomogeneity in the material. Thus, specimens with a steep gradient in carbon content near the surface show overlapping peaks [33, 34]. However, these overlapping peaks were observed equally in tension and compression [34] unlike the compression double peaks (CDPs) observed in the present work. It must be concluded that the CDPs do not arise from inhomogeneity. On the other hand, compression double peaks (CDPs) in homogeneous materials have been reported previously in the literature. Gatelier-Rothea et al. [13] observed double peaks in low carbon iron strained in compression. Similar observations for a low carbon steel were made by Kleber and Vincent [17]. The phenomenon was ascribed to the different effect of stress on 180 and 90° domain walls. Stress acting alone has no effect on 180° walls whilst, because of magnetostriction, compressive stress favours the growth of domains with magnetic vectors at 90° to the stress axis. Thus, the applied field and compressive stress work in opposition for the 90° domains, which therefore tend to be stabilised by compression. On this basis, it is envisaged that the double-peak profiles arise from the movement of the two sorts of domain wall. However, it remains to be explained why double peaks occur with some microstructures under compression but not in others.

Although the mechanism involved in the appearance of the CDPs is not understood in detail, a correlation between their occurrence and lower mechanical strength was noted in a previous paper [22]. That is, CDPs have generally been observed in steels with lower tensile strengths and higher MBN output, i.e.,

materials that are softer in a mechanical and magnetic sense. For instance, CDPs have been reported in low carbon iron [13] and in low carbon steel [17]. These materials have yield strengths under 450 MPa. Profiles with multiple peaks in compression have also been observed in steel with higher carbon content, heat-treated to give a smaller yield strength (spherodised carbide microstructure with σ_0 = 450 MPa), whereas the same material, heat treated to give a higher yield strength, does not exhibit CDPs [22]. The present results fit this pattern only in so far as the lower strength material (OT specimens) shows CDPs, whereas the higher strength material (ST specimens) does not. However, the OT specimens are much stronger than the materials referred to above and it must be concluded that the present results run counter to the previously suggested correlation between CDPs and lower mechanical strength.

Conclusions

The effect of applied stress on the MBN profiles for induction hardened steel specimens with two temper heat treatments (standard temper ST and over temper OT) has been investigated. The following conclusions were made.

(1) With stress in the range –0.25 to $0.5\sigma_0$, where σ_0 is the yield strength, MBN output increases with increasing tension and the output is more sensitive to stress in the OT specimens than in the ST specimens. At higher stresses, output declines with increasing stress. With stresses lower than $-0.25\sigma_0$, output increases slightly with increasing compression.

(2) The MBN profiles for the OT specimens exhibit double peaks under compression while the profiles for the ST specimens exhibit only a single peak. The appearance of double peaks in material under compression is believed to be different responses of 180° and 90° domain boundary walls, although a detailed explanation of the phenomenon cannot be given at the present time.

(3) With the exception of the double peak behaviour described above, the variation of the MBN profile characteristics with stress is broadly consistent with the idea that tension narrows the BH loop of the material while compression broadens the loop.

References

1. Shaw BA, Evans JT, Wojtas AS, Suominen L (1997) Grinding process control using the magnetic Barkhausen noise method. In: Third International Workshop on Electromagnetic Non-Destructive Evaluation. IOS Press in the Series in Applied Electromagnetics and Mechanics; pp 82–91
2. Alessandro B, Beatrice C, Bernotti G, Montorsi AJ (1990) J Appl Phys 68:2901
3. Jiles DC (2000) Czech J Phys 50:893
4. Lo CCH, Lee SJ, Li L, Kerdus LC, Jiles DC (2002) IEEE Trans Magn 38:2418
5. Rautioaho R, Karjalainen P, Moilanen M (1987) J Magn Magn Mater 68:314
6. Rautioaho R, Kivimaa J, Moilanen M (1994) J Magn Magn Mater 129:217
7. Kivimaa J, Moilanen M, Rautioaho R, Zhang H (1993) IEEE Trans Magn 29:2992
8. Sengupta A, Theiner W (1995) Mater Eval 53:554
9. Lindgren M, Lepisto T (2000) NDT & E Int 34:337
10. Iordache VE, Hug E, Buiron N (2003) Mat Sci Eng A 359:254
11. Jagadish C, Clapham L, Atherton D (1990) IEEE Trans Magn 26:1160
12. Hyde TR, Evans JT, Shaw BA (2000) Mater Eval 58:985
13. Gatelier-Rothea C, Chicois J, Fougres R, Fleichman P (1998) Acta Mater 46:4873
14. Stefanita CG, Atherton DL, Clapham L (2000) Acta Mater 48:3545
15. Anglada-Rivera J, Padovese LR, Capó-Sántchez J (2001) J Magn Magn Mater 231:299
16. Pérez-Benitez JA, Padovese LR, Capó-Sántchez J, Anglada-Rivera J (2003) J Magn Magn Mater 263:72
17. Kleber X, Vincent A (2004) NDT & E Int 37:439
18. Stewart D, Stevens K, Kaiser A (2004) Curr Appl Phys 4:308
19. Parakka A, Jiles DC, Gupta H, Jaliccs S (1996) J Appl Phys 79:6045
20. Parakka AP, Jiles DC, Gupta H, Zang M (1997) J Appl Phys 81:5085
21. Sipahi L, Devine M, Jiles DC, Palmer D (1993) Rev Prog Qua Non Dest Eval 12:1847
22. Blaow M, Evans JT, Shaw BA (2005) Acta Mater 53:279
23. Blaow M, Magnetic Barkhausen Noise in Steel, Ph.D. Thesis University of Newcastle upon Tyne, 2005
24. Blaow M, Evans JT, Shaw BA (2004) Mater Sci Eng A 386:74
25. Timoshenko S, Young DH (1968) Elements of strength of materials. Van Nostrand, Princeton NJ
26. Birkbeck G, Petch NJ, Rae DM (1972) J Iron Steel Inst 210:675
27. Jiles DC, Suominen L (1994) IEEE Trans Magn 30:4924
28. Jiles DC, Sipahi LB, Williams G (1993) J Appl Phys 73:5830
29. Sablik MJ (1993) J Appl Phys 74:5898
30. Jiles DC (1988) J Phys D: Appl Phys 21:1186
31. Sablik MJ, Augustyniak B (1996) J Appl Phys 79:963
32. Sablik MJ, Jiles DC (1993) IEEE Trans Magn 29:2113
33. Blaow M, Evans JT, Shaw BA (2005) J Mater Sci 40:5517
34. Blaow M, Evans JT, Shaw BA (2006) J Magn Magn Mater 303:153